

## REVIEW ARTICLE



# The chronicles of coronaviruses: the electron microscope, the doughnut, and the spike

**K. Lalchandama**

Department of Life Sciences, Pachhunga University College, Aizawl 796001, India

The advancement of medicine owes in large measure to a German engineer Ernst Ruska, whose invention of transmission electron microscope in 1931 won him the 1986 Nobel Prize in Physics, when it comes to infectious diseases. Encouraged by his physician brother Helmut Ruska to use the prototype instrument for the study of viruses, the course of virology was shifted to a different and unprecedented level. Virus could then be seen, identified and imaged. The University of Maryland happened to acquire an American model of transmission EM, the RCA EMU, using which the first structural study was done for the first known coronavirus (then was simply known as infectious bronchitis virus) in 1948. The virus was described as rounded bodies with filamentous projections. The magnification was not great and the resolution was poor. The study was followed by a series of studies using improved techniques and better EM spanning the next decade. An upgraded version RCA-EMU2A gave better images in 1957 and the virus was described as doughnut-like structure. Using Siemens Elmiskop, D.M. Berry and collaborators made the first high-resolution pictures in 1964. The thick envelope which gave doughnut-like appearance and filamentous projections reported before could be discerned as discrete pear-shaped projections called the spikes. These spikes form a corona-like halo around the virus, which were also seen in novel human viruses (B814 and 229E) that caused common colds. The discoverer of B814, David Tyrrell and his aid June Almeida, a magnificent electron microscopist, established that IBV, B814 and 229E were of the same kind of virus in 1967, which prompted to create the name coronavirus in 1968. This article further highlights the detail structural organisation of coronaviruses emanating from these pioneering research.

Received 11 May 2020  
Accepted 29 May 2020

\*For correspondence:  
[chhandama@pucollege.edu.in](mailto:chhandama@pucollege.edu.in)

Contact us:  
[sciencevision@outlook.com](mailto:sciencevision@outlook.com)

**Keywords:** Coronavirus, electron microscope, envelope, spike, genome

## Invention of Electron Microscope – The German Efficiency

Ernst August Friedrich Ruska had earned his Diplom-Ingenieur (Diploma in Engineering) from the Technische Hochschule zu Berlin (Technical University of Berlin) in 1931. His dissertation titled

*“Untersuchung elektrostatischer Sammelvorrichtungen als Ersatz der magnetischen Konzentrierspulen bei Kathodenstrahl-Oszillographen (Investigation of electrostatic concentrating devices as a substitute for the magnetic concentrating coils in cathode ray oscillographs)”* was supervised by Max Knoll. Knoll had been an expert in the field and filed patent a

method of arranging electron beams of a cathode ray oscilloscope in 1929. Ruska was trying to improve the device in his dissertation. After submitting his dissertation on 23 December 1930, he soon realised that he committed a serious mistake which Knoll did not know. As he later recapitulated,

I overlooked that as a consequence of the considerably varying electron velocity on passage through such a field arrangement [the electrodes on either side of the lens centre] a concentration of the divergent electron bundle must, in fact, occur. Knoll did not notice this error either.<sup>1,2</sup>

At the peak of the Great Depression, there was no job opportunity but he luckily got an enrolment as a doctorand (student of Doktoringenieur, or Doctor of Engineering). After a few months, he was able to find out the problem. By April, he was holding in his hands what he called "electron lens." He described the implications as

After having shown, in my Studienarbeit of 1929, that sharp and magnified images of electron-irradiated hole apertures could be obtained with the short coil, I was now interested in finding out if such images—as in light optics—could be further magnified by arranging a second imaging stage

behind the first stage. Such apparatus with two short coils was easily put together and in April 1931 I obtained the definite proof that it was possible. This apparatus is justifiably regarded today as the first electron microscope even though its total magnification of about  $3.6 \times 4.8 = 17.4$  was extremely modest.<sup>1,2</sup>

His first experiment on 7 April 1931 gave the first electron microscopic images (of the aperture grids). He published the scientific principle in 1932.<sup>3</sup> Thus was born the electron microscope (**Figure 1**). But then the resolving power was no better than that of a light microscope, and thus had no practical value. In 1932, Knoll left him for a new position at Telefunken, a radio and television apparatus company in Berlin. His means were restrained, but was luckily funded, as he comically recalled:

To carry out this task [of improving the resolution] I obtained, by the good offices of Max v. Laue, a stipend of 100 Reichmarks per month for the second half year of 1933 from the Notgemeinschaft der Deutschen Wissenschaft to defray running costs and personal expenses. Since I had completed the new instrument by the end of November, I felt I ought to return my payment for December. To my great joy, however, I was allowed to keep the money "as an exception". Nevertheless,

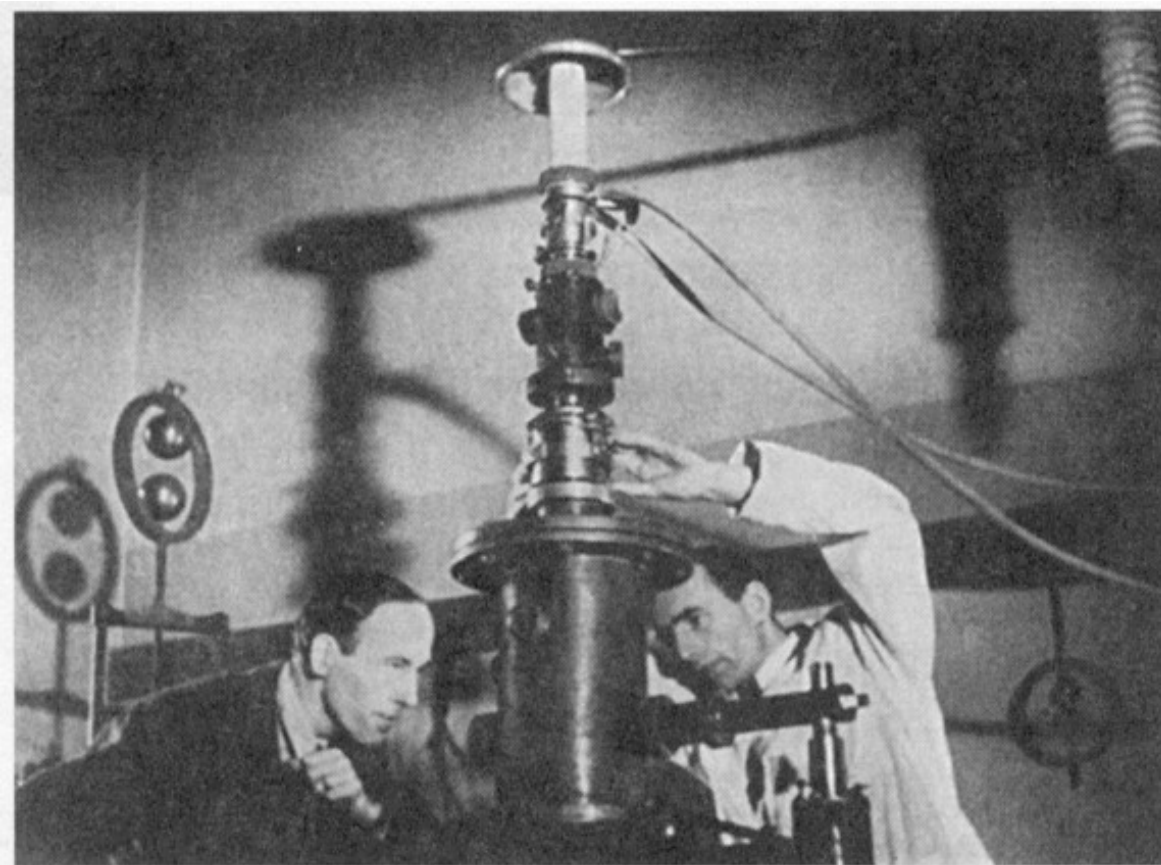


**Figure 1** | The first electron microscope being carefully checked by Ernst Ruska (right), as Max Knoll (left) keenly observed in 1931.



**Figure 2** | The first prototype of electron microscope built by Ernst Ruska in 1933.

this certainly was the cheapest electron microscope ever paid for by a Deutsche Gesellschaft für Wissenschaftsförderung (German Society for the Promotion of Science).<sup>1,2</sup>

His new improved lens, with several hundred times more ( $\times 12,000$ ) resolution than his original,<sup>4</sup> was clearly of a huge potential (**Figure 2**).

His brother Helmut Ruska, a medical student, was among the firsts to realise the possible application in biology. With Helmut and brother-in-law Bodo von Borries, who were by then working at the Siemens-Reiniger-Werke AG, he applied for funds to different companies and government for constructing make a commercial electron microscope. As the biological applications became more and more convincing after the studies of Heinz Otto Müller and Friedrich Kraus,<sup>5</sup> as well as by Ladislaus Marton in Belgium,<sup>6</sup> Siemens agreed to finance in 1937. Then, Helmut was relieved from Charité (the Director Richard

Siebeck was a key expert who recommended the funding in the first place, and it was apparent that Helmut had convinced Siebeck in his decisions), where he was a physician, to join the new laboratory.<sup>7</sup> Within one year they made the first two prototypes having magnification of  $\times 30,000$ , which were later known by the generic name conventional transmission electron microscopes.<sup>8</sup> Helmut used one of the prototypes to study viruses, which could not be seen with light microscope, with huge success.<sup>9</sup> The rest, as they say, is history.

Ruska's doctoral thesis titled "*Über ein magnetisches Objektiv für das Elektronenmikroskop* (On a magnetic objective lens for the electron microscope), submitted on 31 August 1933, and published in 1934<sup>10</sup> would have mattered little for the 1986 Nobel Prize in Physics for his invention (**Figure 3**). His invention paved a new way in virology, to say the least.



**Figure 3** | Ruska (left) receiving the Nobel Prize from King Carl XIV Gustaf of Sweden in 1986.

### Unveiling the Faces of Invisible Viruses

The invention and subsequent development of electron microscopes was a boon to biology and revolutionised the study of microorganisms, particularly viruses, which were otherwise totally invisible until then. RCA (Radio Corporation of America), headed by Russian engineer Vladimir Zworykin, was the first to make electron microscope model EMU (**Figure 4**) was made by RCA (Radio Corporation of America) since in US in 1939. In 1944 and was the first microscope they manufactured in US an improved model EMU which was the first microscope capable of both imaging and electron

diffraction. Using this equipment at the University of Maryland Reginald L. Reagan, Jean E. Hauser, Mary G. Lillie, and Arthur H. Craig Jr. were the first to show the structure of corona virus (in their case infectious bronchitis virus or *Avian coronavirus*) in 1948 (**Figure 5**). They cultured IBV in embryonated eggs and isolated them in the allantoic fluid. At magnification  $\times 25,000$  the viruses appeared no more than ink spots on a sheet of paper. But the description was very useful for later identification of other coronaviruses. The virions appeared spherical and measured between 65 and 135 nm, and more notably most of them showed fuzzy hair-like projections around them. As the paper concluded:

Electron micrograph studies of the virus of infectious bronchitis of chickens revealed virus particles round in shape. A small percentage of the bodies had a filamentous projection, similar to that described for Newcastle disease virus. The virus of infectious bronchitis used in these electron studies appeared serologically distinct from that of Newcastle virus.<sup>11</sup>

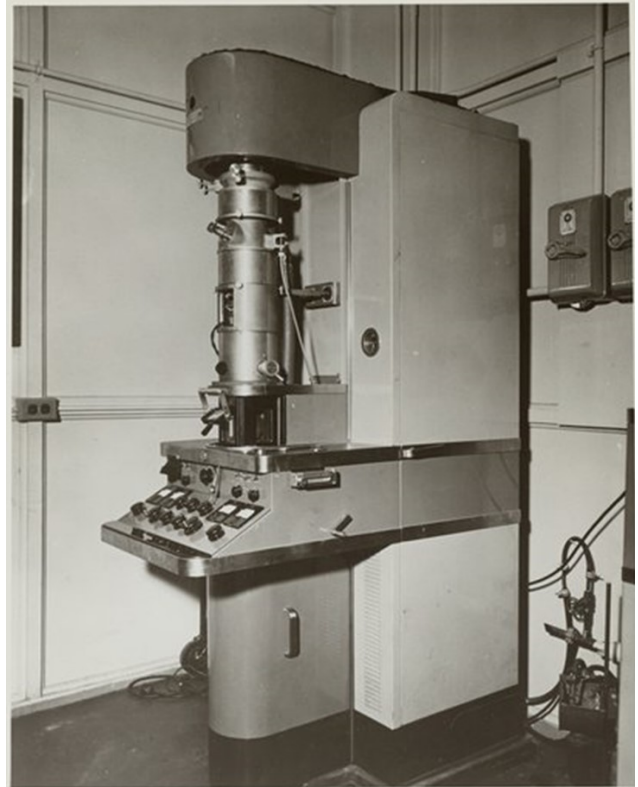


**Figure 4** | RCA Model EMU electron microscope in the Aeronautical Materials Laboratory, USA, in 1958.

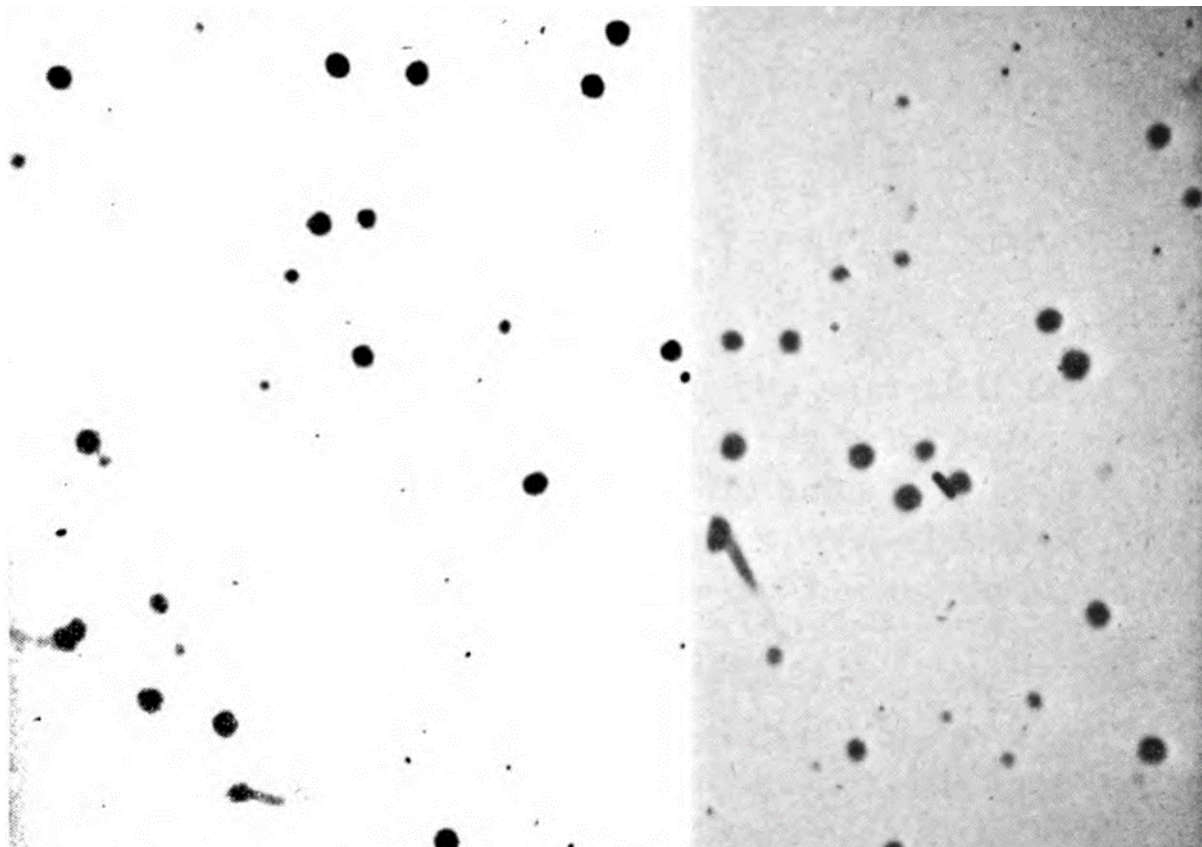


**Figure 5** | The first image of coronavirus (infectious bronchitis virus or *Avian coronavirus*) taken with electron microscope in 1948 by Reagan *et al.*<sup>11</sup>

subsequent studies on the same virus with improved technique on virus isolation gave slightly better images but not sufficient to describe the other details.<sup>12,13</sup> They showed no particular distinction from those of other viruses.

The images at  $\times 12,000$  to  $\times 58,000$  magnifications made by Charles Henry Domermuth and O.F. Edwards at the University of Kentucky in 1957 using RCA-EMU2A created a bit of confusion. They failed to notice any projections as described by Reagan and co-workers. But what they missed is that due to very poor preparation their images showed thick outer layer with a central hollow space and gave a description as "a thick ring or doughnut-like structure". For this reason, their measurement indicated IBV was quite large, 178 to 200 nm diameter. It could have been an evidence of the projections that made the envelope extra thick. But they could describe briefly of the internal structure (nucleic acid and nucleocapsid) as "rows of electron transparent spots which are about 20  $\mu\text{m}$  in diameter. Within some of the spots there is an electron dense body of smaller diameter."<sup>14</sup>

As the resolutions of electron microscopy were gradually improved, the images got better and better. The first high-quality images of IBV were produced by D.M. Berry at the Glaxo Laboratories in Middlesex, UK, and collaborators at the University of Cambridge, in 1964. Their electron microscope Siemens Elmiskop was a highly improved model. At magnification as high as  $\times 200,000$  the unique structural organisations began to be revealed. Four strains of IBV were compared, and in contrast to the images of Domermuth and Edwards, all of them exhibited surface projections. In fact, the structure of the projections were described in detail for the first time. Introducing the term "spikes" for the projection, the description was given as:

The particles showed considerable pleomorphism although most of them were approximately circular in outline with diameters between 80 and 1200 Å [= 80 and 120 nm]. Most but not all of the particles had projections from their surfaces. These "spikes" were often seen over part of the surface only and were less densely packed than those seen in influenza viruses. They varied considerably in shape. Commonly they appeared to be attached to the virus by a very narrow neck and to thicken towards their distal ends, sometimes forming a bulbous mass 90-110 Å in diameter. These pear-shaped masses could sometimes be seen lying on the surface of particles, apparently in clusters. In other particles the spikes were more rod-shaped, but many were bent in the middle.<sup>15</sup>

Another important observation was that treatment of the viruses with sodium dodecyl sulphate destroyed the spikes, indicating that the spikes were made of proteins. It was more than clear that IBV was a stranger among the known viruses, as the study was aptly concluded:

Infectious bronchitis thus shows certain unique features morphologically as well as biologically, and recognition of its true position in virus classification must wait until further information is forthcoming.<sup>15</sup>

José Francisco David-Ferreira and Robert A. Manaker from the National Cancer Institute, Bethesda, studied mouse hepatitis virus (MHV) using Siemens Elmiskop I in 1965. At magnifications ( $\times 20,000$  to 120,000), the resolution was very high. The viruses as they progressively infect mouse liver cells could be clearly seen. It was an evidence of the viral entry into host cells by the process of phagocytosis. The budding virus showed a sharp picture of an arc of surface projections. They referred to the projections as "spicules".<sup>16</sup>

An unusual virus that caused common cold was found in Epsom, Surrey, England. David Arthur John Tyrrell and his team at the Common Cold Research Unit collected nasal swab samples from schoolboys in boarding schools who had common colds during 1960-61. Some samples they found could not be cultured in any of the culture methods used for cold viruses, indicating that the pathogen could not be the usual cold viruses.<sup>17</sup> They experimented one sample, designated B814, collected from one boy on 17 February 1961, by infecting healthy volunteers. It was exceptionally contagious when they inoculated to healthy volunteers and they wondered whether the cold agent was a virus or a bacterium. It was only in 1965 that they were able to grow the pathogen in a modified culture media using human-embryo-trachea epithelial cells, a technique devised by a Swedish surgeon Bertil Hoorn. They could now isolate and identify it as a virus.<sup>18</sup>

To show that the new cold virus was not an accidental or abnormal virus, Dorothy Hamre and John J. Procknow at the Department of Medicine, University of Chicago obtained a sample, which they labelled 229E, from a medical student having a cold in 1962. They isolated the virus after culturing in a secondary human kidney tissue in 1966.<sup>19</sup> With David A. Kindig and Judith Mann, Hamre studied the growth pattern of 229E in human diploid cells (WI-38) using fluorescent and electron microscope. After 6 hours of infection, the viruses emerged as spherical bodies and at 12 hours the virus structure was very clear. The 6 hour sample was nicely described as:

The particles were spherical, 80 to 100  $\mu\text{m}$  in diameter, and contained a "hollow" or electron-transparent central area 35 to 50  $\mu\text{m}$  diameter. Beneath the outer surface and delineating the hollow core was an electron-dense ring. This ring was not always the same thickness at all points of its circumference, but varied from 5 to 10  $\mu\text{m}$  to virtually nothing.<sup>20</sup>

Their images were not as good as those of David-Ferreira and Manaker, otherwise they would not have failed to describe the electron-dense ring as

projections, i.e. the spikes.

Tyrrell at this moment was immersed in a quandary over how to propagate and properly identify the new virus. He approached Anthony Peter Waterson, who was recently appointed professor of virology at the St Thomas's Hospital Medical School in London. St Thomas's had an electron microscope Philips 200 for which Waterson had just recruited a young Scottish microscopist June Almeida. Almeida had been a technician at the Ontario Cancer Institute, University of Toronto, Canada, where she had developed two vital techniques for electron microscopy in virology in 1963: One was a negative staining method which she modified using phosphotungstic acid and carbon-coated Formvar grid,<sup>21</sup> and the other was antigen-antibody conjugation method in which she made antigen (virus) bound to antibody (from goat or rabbit) to create antigen-antibody complex.<sup>22</sup>

Tyrrell a little faith over Almeida's technique but Almeida was perfectly confident. Almeida had the right to her confidence because she already had studied IBV and MHV, the paper on which was sadly rejected by a journal whose referee commented that the electron microscopic images were those of influenza viruses badly focussed. (She published the IBV data anyway later in *Journal of General Virology* in 1968.<sup>23</sup>) Tyrrell asked from Hamre a sample of 229E, and with B814 he sent them to Almeida. As the images were produced (**Figure 6**), Tyrrell was far from being disappointed, as he exclaimed:

The results exceeded all our hopes. She recognised all the known viruses, and her pictures revealed their structures beautifully. But, more importantly, she also saw virus particles in B814 specimens!<sup>24</sup>

The uncanny resemblance between B814 and 229E and IBV was overwhelming. They all had the basic spherical shape with a diameter of 80 to 120 nm. The surface projections were 20 nm long from the surface. Each projection had a lollipop-like appearance with a thin stalk and a globular tip they called the "head", which was 10 nm in diameter. In their report of 1966 published in the *British Medical Journal* in 1967, Almeida and Tyrrell remarked:

Probably the most interesting finding from these experiments was that two human respiratory viruses, 229 E and B814 are morphologically identical with avian infectious bronchitis. Their biological properties, as far as they are known, are consistent with this. Both the human viruses are ether sensitive as is avian infectious bronchitis 229 E, have a similar size by filtration and multiply in the presence of an inhibitor of DNA synthesis".<sup>25</sup>

As the identity of these viruses including MHV and novel human virus (**Figure 7**) as a single group was further supported independently,<sup>26,27</sup> it did not take long for Tyrrell and Almeida to come up with the new name, coronavirus, as Tyrrell reminisced:

Even though we could only base our judgement on the electron microscope images we were quite certain that we had identified a previously unrecognised group of viruses. So what should we call them? 'Influenza-like' seem a bit feeble, somewhat vague, and probably misleading. We looked more closely at the appearance of the new viruses and noticed that they had a kind of halo surrounding them. Recourse to a dictionary produced the Latin equivalent, corona, and so the name coronavirus was born.<sup>24</sup>

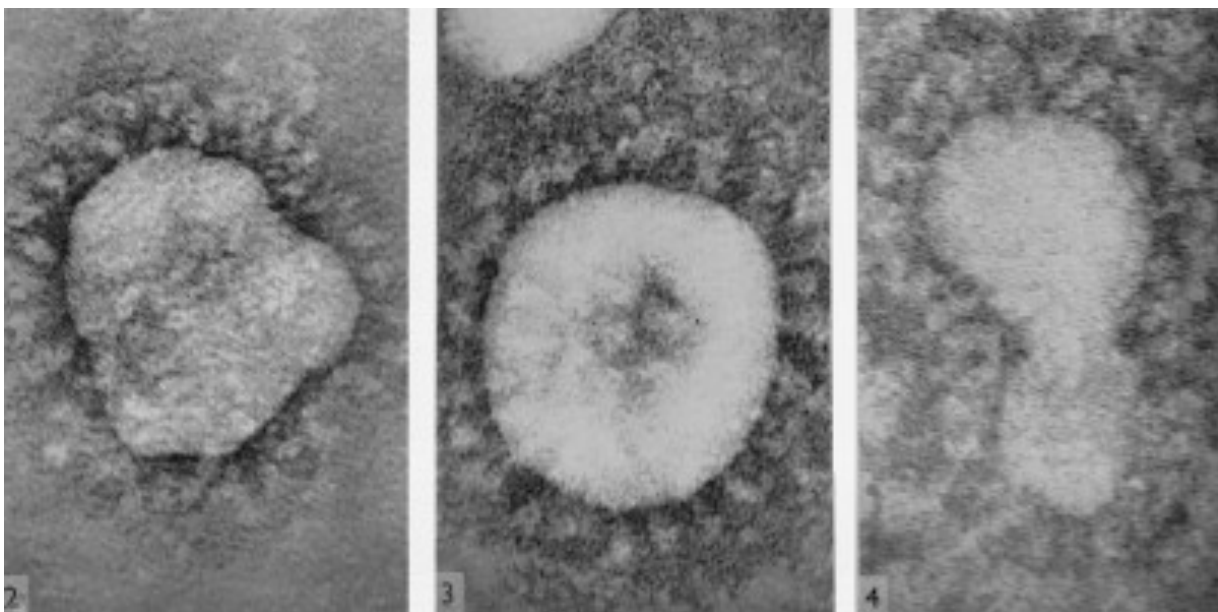


**Figure 6** | The first human coronavirus coronaviruses 229E (2) and B814 (3&4) taken by June Almeida in 1966.<sup>11</sup>

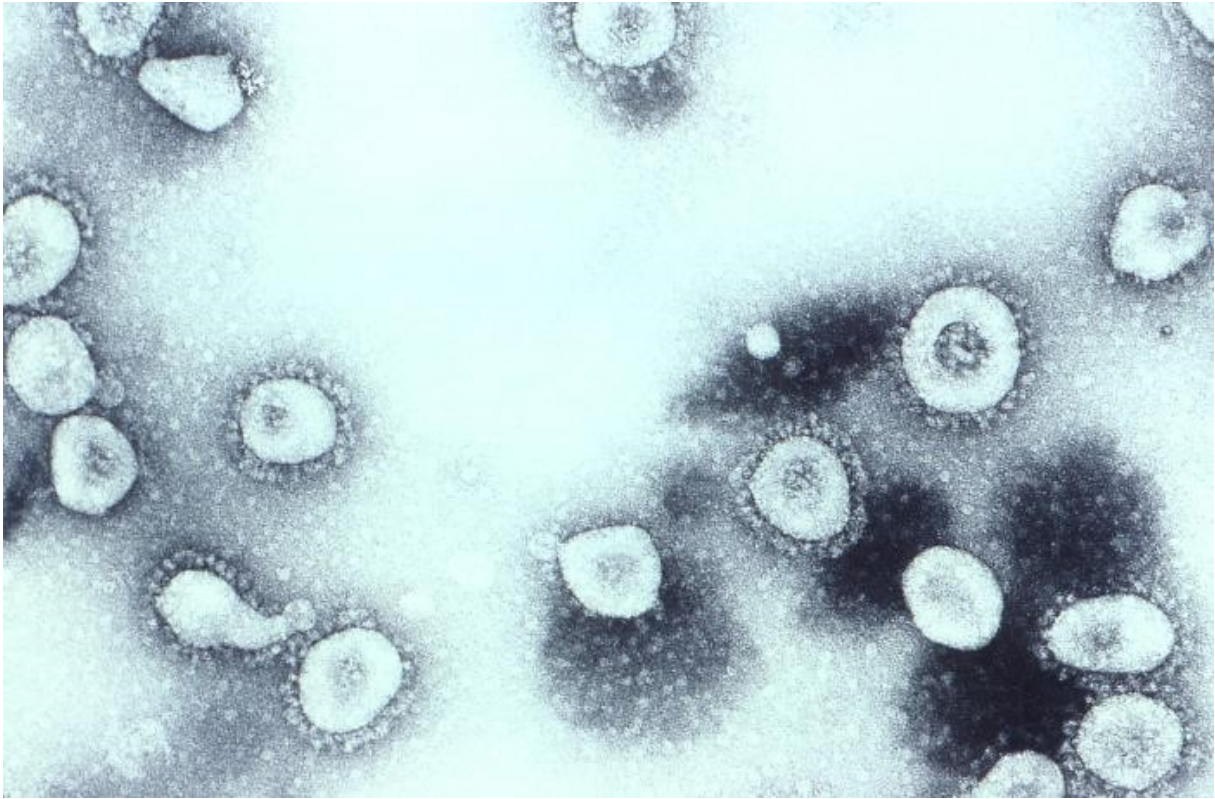


**Figure 7** | Human coronavirus OC43 image taken in 1981. (CDC)

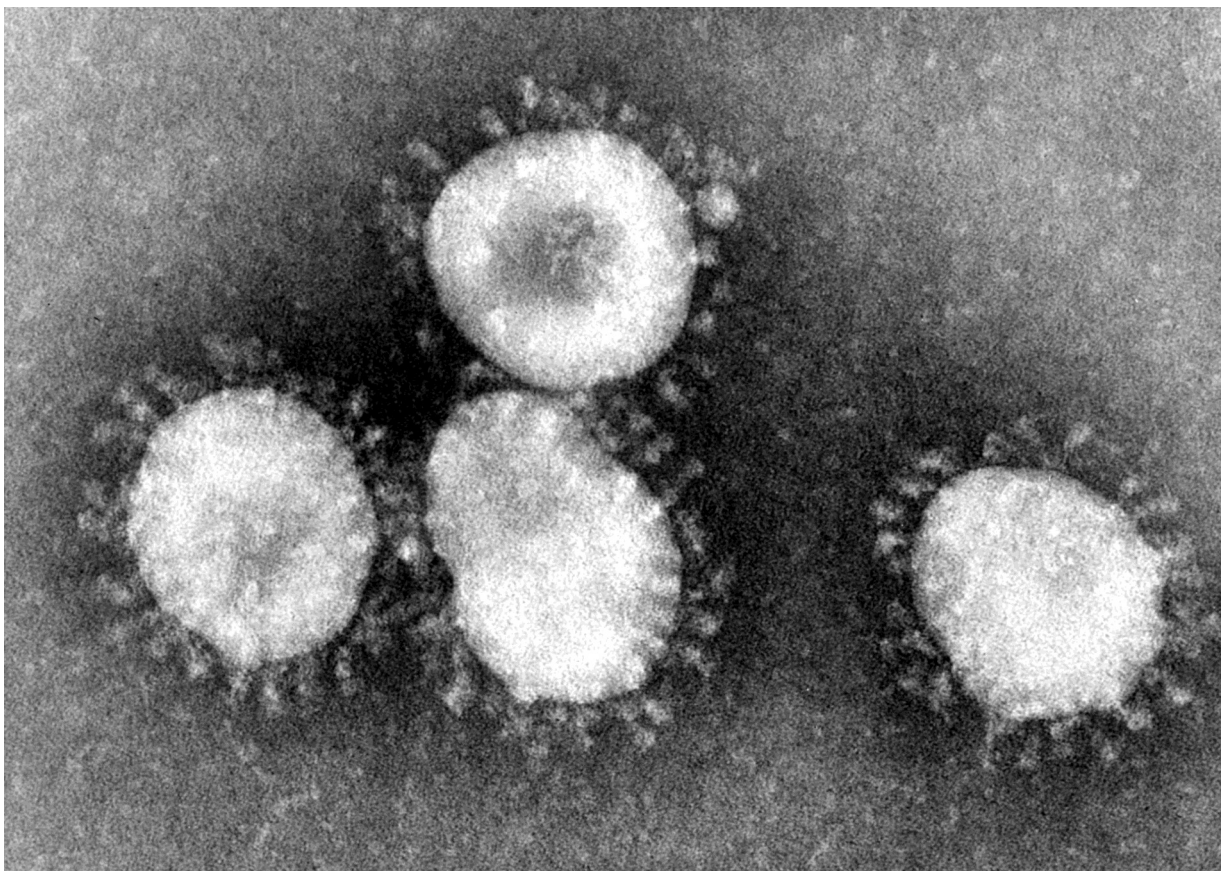


**Figure 8** | Infectious bronchitis virus (*Avian coronavirus*) image taken in 1975. (CDC)

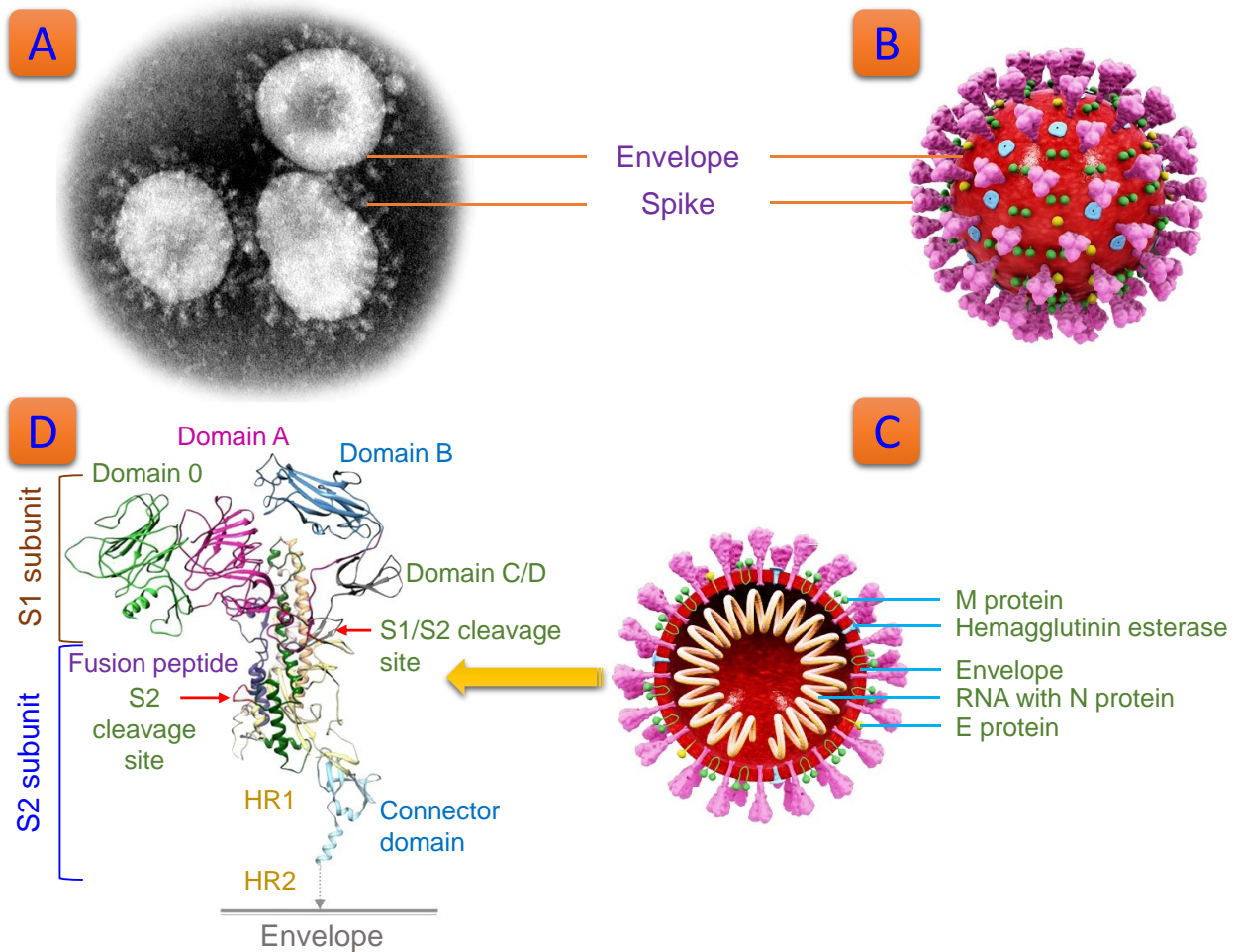


**Figure 9 |** Structure of coronaviruses. A. Transmission electron micrograph of infectious bronchitis viruses (IBVs) from chicken. B & C. Structural models of typical CoV; note that hemagglutinin esterase is absent in SARS-CoV and SARS-CoV-2. D. Atomic model of a single spike of feline infectious peritonitis virus (FIPV) based on cryo-electron microscopy. HR = heptad repeats.

**General Structure**

Coronaviruses (CoVs) are pleomorphic particles in that different species exhibit unique structural component and organisation. However, they all have the same fundamental architecture (Figures 6–8). The variation lies in the type of amino acids and how the genes for these operate and align. A typical CoV is spherical in shape and measures approximately 120 to 160 nm in diameter and 40,000 kDa in size. SARS-CoV-2 is quite variable in shape and size. Seen mostly as spherical but sometimes oblong, size ranges from 60 to 140 nm in diameter.<sup>28</sup> All CoVs are entirely covered by a proteinaceous envelope, inside of which lies the nucleic acid, and RNA molecule. The physical integrity is maintained by four structural proteins: membrane (M) protein, envelope (E)

protein, nucleocapsid (N) protein, and spike (S) protein (Figure 9).<sup>29,30</sup>

*The envelope – a coat of many colours*

The skeletal framework of the envelope is made up of a single major structural protein, which is a type III membrane (M) protein. An M protein consists of 218 to 263 amino acid residues. For a virus that tiny, the M protein forms a remarkably thick layer, at 7.8 nm. It has three domains: a short amino- or N terminal ectodomain, a triple-spanning trans-membrane domain, and a C-terminal domain. The envelope-embedded portion of the proteins, the C-terminal domain, appears to form a matrix-like lattice, which apparently is the reason for the extra-thickness of the envelope. The externally exposed

portion of the proteins are called amino-terminal domain. Different species can have either *N*- or *O*-linked glycans in their proteins in amino-terminal domain. The M protein is crucial in the life cycle of the virus such as during assembly, budding, envelope formation, and pathogenesis.<sup>31</sup>

The M protein is highly susceptible to degradation under heat, lipid solvents, non-ionic detergents, formaldehyde, oxidizing agents and ultraviolet irradiation. This is the basis of washing hand frequently with any kind soap as the best and most practical measure for warding off of the viruses on the skin. It is quite conserved among CoVs, but at least seven variants are known in SARS-CoV-2.<sup>32</sup>

Studded among the M proteins are the envelope (E) proteins. The E proteins are minor structural proteins of the envelope and are highly conserved among members of *Betacoronavirus*. They are most abundant in infected cells, but less so in virions. In infected cells, they are localised in the intracellular membranes between endoplasmic reticulum and Golgi compartments.<sup>33</sup> This explains their interaction with lipid layers only after infection. They are responsible for virion assembly, intracellular trafficking and morphogenesis (budding). They act as ion channels and membrane permeabilizing proteins (vioporins). They are composed of pentameric integral membranes having 74 to 109 amino acid residues. They have (at least) two distinct domains namely transmembrane domain and extramembrane C-terminal domain. In MERS-CoV and SARS-CoV, an E protein is almost fully  $\alpha$ -helical, with a single  $\alpha$ -helical transmembrane domain, and forms pentameric (five-molecular) ion channels in lipid bilayers.<sup>34</sup> In a single CoV there are about 20 E proteins, which are specifically distributed at the ER-Golgi intermediate compartment (or ERGIC). In SARS-CoVs, in addition to performing the basic functions, the E proteins act as virulence factors,<sup>35</sup> and transport calcium ions ( $\text{Ca}^{2+}$ ). Acting as  $\text{Ca}^{2+}$  channels they initiate activation of caspase-1 and maturation of pro-inflammatory IL-1 $\beta$  during infection.<sup>36</sup>

### *The spike – the weapon of mass destruction*

The most notable and distinguishing structural component of CoVs is the presence of tiny club- or petal-shaped projections having their thin stalk anchored to the surface of the virus. These projections are referred to as the “peplomers” or “spikes”. The spherical distribution of these projection all over the viral surface renders the virus to have a halo-like appearance, something like the corona of the Sun, and hence the name coronavirus.<sup>24,37</sup> *Corōna* is a Latin for garland or crown. The spikes are 15 to 20 nm in diameter, and each is made up of three molecules (trimer) of type I glycoproteins. The spikes of SARS-CoVs are the smallest, measuring about 9 to 12 nm in diameter.<sup>28</sup>

Each spike (S) protein comprises 1128 to 1472 amino acid residues. The S protein is highly glycosylated containing 20 to 35 *N*-linked glycans. The protein is cleaved into two subunits, S1 and S2, by cytoplasmic protease. The two subunits remain noncovalently linked as they are exposed on the viral surface, until they attach on the host cell membrane.<sup>29,30</sup> However, the S proteins of the alphacoronaviruses remain as a monomer and are not cleaved. Remarkably, in Human CoV-NL63, an alphacoronavirus, binding to the host cell is independent of the S proteins; instead, the region of the M protein spanning 153 to 226 amino acid residues act as the binding site.<sup>40</sup>

Each spike is made up of three structural domains, namely a large ectodomain, a single-pass transmembrane domain, and a short intracellular tail. The S1 and S2 subunits make up the ectodomain. The S1 subunits are the receptor-binding sites of CoVs, and contain a signal peptide, followed by an N-terminal domain (NTD) and receptor-binding domain (RBD). Whereas the S2 proteins are responsible for fusion of the viral envelope with that of the host cell, and contain conserved fusion peptide (FP), heptad repeat (HR) 1 and 2, transmembrane domain (TM), and cytoplasmic domain (CP).<sup>41</sup> Three S1 proteins constitute the globular structures of the spikes. They contain sequences necessary for receptor recognition on the surface of the host cells and subsequent fusion with the host cell membrane to initiate entry of the virus into the cell. As such they are responsible for the pathogenicity and immunogenic properties of the virus. The three S1 proteins are attached to two S2 proteins. The small transmembrane domain acts as anchorage of S2 on the viral surface, and is exposed on the inside of the virus as an intracellular tail.<sup>30</sup> As the virus binds and fuses with the host cell, proteases including members of the cathepsin family and transmembrane protease serine 2 (TMPRSS2) of the host cell cleaves the S protein to their subunits.<sup>42</sup>

S1 proteins are the most crucial parts of CoV as they serve as direct recognition and interaction sites for the host cells. They are also the most variable components in CoVs and are responsible for host specificity. There are two major domains in S1 named N-terminal domain (S1-NTD) and C-terminal domain (S1-CTD). They are the receptor-binding domains (RBDs). The NTDs recognise and bind sugars on the surface of the host cell. The bovine coronavirus (BCOV) NTD recognizes 5-*N*-acetyl-9-*O*-acetylneuraminic acid on the host cell. An exception is MHV NTD that binds to a protein receptor carcinoembryonic antigen-related cell adhesion molecule 1 (CEACAM1).<sup>43</sup> S1-CTDs are responsible for recognizing different protein receptors such as angiotensin-converting enzyme 2 (ACE2), aminopeptidase N (APN), and dipeptidyl peptidase 4 (DPP4).<sup>39</sup> For this reason, CoVs are able to attack different cells and tissues. For instance, SARS-CoVs bind to ACE2, which are expressed on the cells of

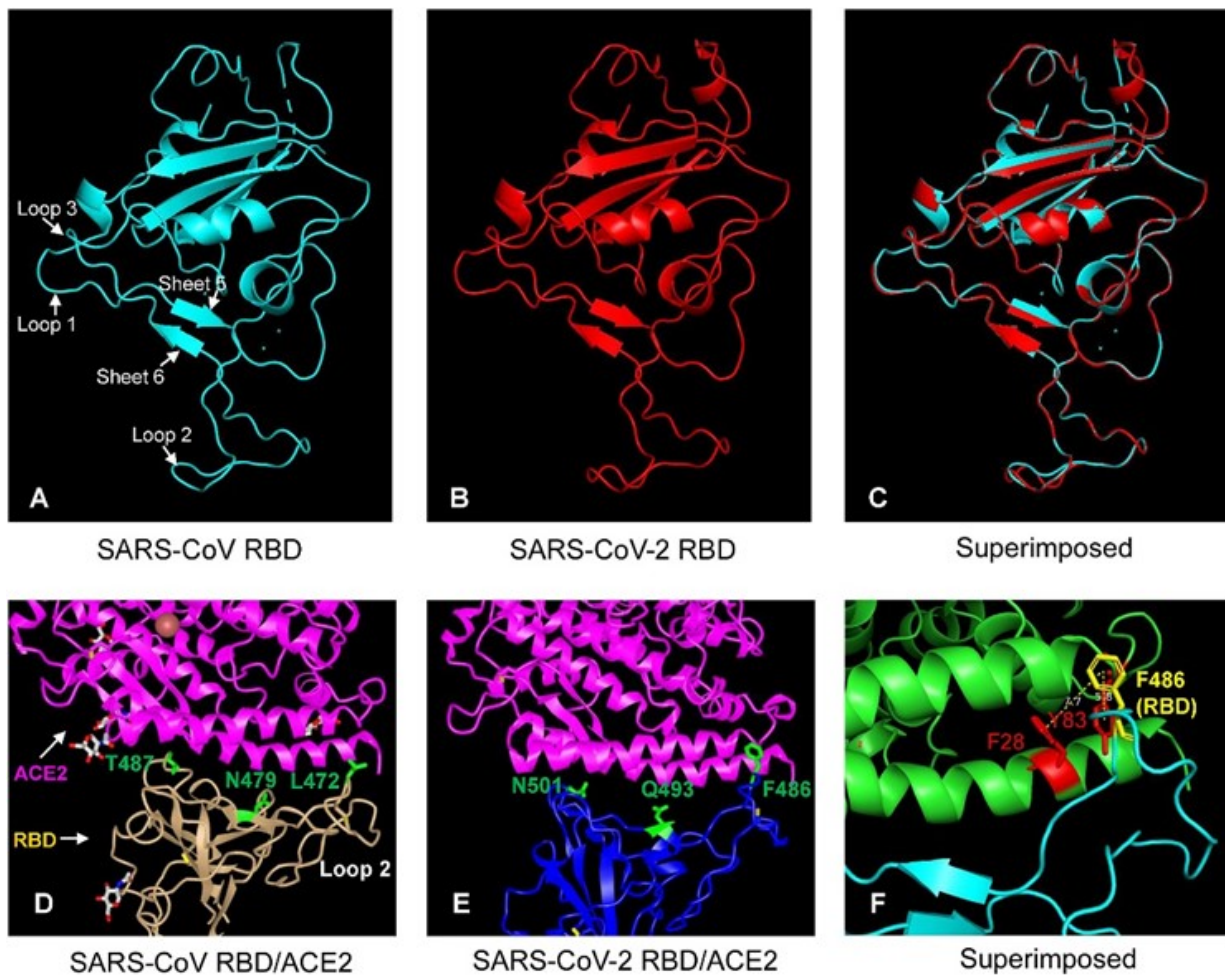


**Figure 10** | Molecular models of the receptor-binding domains (RBDs) of SARS-CoV and SARS-CoV-2. Both bind to angiotensin-converting enzyme 2 (ACE2) on human cells. Thus, they are the most crucial sites for pathogenesis in the host as well as targets for drug and vaccine.

adipose tissue, gall bladder, heart, intestine, kidney, ovary, respiratory tract, testis, and thyroid glands. Thus, they are able to produce multiple and more complex symptoms in different organs.

Six amino acids in the RBD determines the receptor-binding affinity for CoVs, although the amino acid in each species is highly variable. For instance, SARS-CoVs (**Figure 10**) and Human CoV-NL63 are known to have high affinity for angiotensin-converting enzyme 2 (ACE2) in humans. But for specific binding to ACE2 receptor, they use different amino acids. In Human CoV-NL63 the core RBD is composed of Lys-353, Phe-493, Tyr-498, Ser-535, Trp-541, and Trp-585;<sup>44</sup> in SARS-CoV, Tyr-442, Leu-472, Asn-479, Asp-480, Thr-487 and Tyr-4911; while it is Leu-455, Phe-486, Gln-493, Ser-494, Asn-501 and Tyr-505 in SARS-CoV-2.<sup>45,46</sup> Overall, the RBDs in SARS-CoV-1 and SARS-CoV-2 share 72% identity in amino acid sequences. SARS-CoV-2 has higher binding affinity for ACE2. In contrast to SARS-CoV-1, SARS-

CoV-2 contains a distinct loop with flexible glycylic residues. The Phe-486 of the flexible loop may be the factor for higher binding affinity as it is able to insert more deeply into the hydrophobic pocket in ACE2.<sup>47</sup> ACE2 is a ubiquitous and conserved protein in vertebrates, forms fishes to humans. Thus, it is more than plausible that SARS-CoV-2 would bind with high affinity to non-human ACE2 such as those of pigs, primates, ferrets and felines, because of high homology of their receptors.<sup>45</sup> Cats are especially highly susceptible to airborne infection with the virus.<sup>48</sup> This capacity of SARS-CoV-2 to cross multi-spectrum hosts was confirmed by the fact cats, dogs and a four-year-old female Malayan tiger, named Nadia, at the Bronx Zoo New York City, have been infected by the virus.<sup>49</sup>

Members of group A *Betacoronavirus* have an additional surface projection composed of homodimeric (two similar molecules) glycoproteins called haemagglutinin-esterases (HEs). The HEs of

CoVs are class I envelope proteins. They are made up of about 400 amino acid residues and are 40-50 kDa in size. They appear as tiny surface projections of 5–7 nm long embedded in between the spikes.<sup>50</sup> They are also heavily glycosylated and contain 5 to 11 N-linked glycans. The HEs promote both attachment to and detachment from target cells. Acting as lectins, they bind to 9-O-acetylated sialic acids and as sialate-O-acetyl esterase, they act as receptor-destroying enzymes.<sup>51</sup> Uniquely, HEs are absent in SARS-CoV and SARS-CoV-2,<sup>41</sup> indicating they are not essential components for structural integrity nor are they crucial in pathogenicity of the CoVs.

**The capsid – guardian of the genome**

The nucleocapsid separates the nucleic acid from the envelope by maintaining a 4-nm space. The nucleocapsid is made up of an RNA-binding phosphoprotein, which consists of 349 to 470 amino acid residues. The nucleocapsid (N) protein and the underlying RNA are arranged in a helical strand. Unlike in other viruses, the nucleocapsid is loosely twisted. The N protein has a multifaceted role: it guards the nucleic acid, aids RNA synthesis and translation, serves as RNA chaperone, and as a type I interferon antagonist.<sup>52</sup> It is structurally organised

into two highly conserved major domains, namely the N-terminal domain (NTD/ N1b) and the C-terminal domain (CTD/ N2b). The two domains are flanked by the minor domains, N1a domain at the N-terminal end, N2a domain in the middle, B spacer in between N2a and N2b, and N3 domain at the C-terminal end.<sup>53</sup> Dimerisation occurs only at the CTD. There is a linker region in between the NTD and CTD and is rich in serine and arginine residues. The nuclear localization signal (NLS) is located at the terminal end of CTD. The NTD associates with the 3' end, and the CTD with the 3' end of the viral RNA genome.<sup>54</sup> The NTD is rich in aromatic and basic amino acid residues and the folded molecule resembles a hand with basic fingers that extend far beyond the protein core, a hydrophobic palm, and an acidic "wrist". The flexible, positively charged finger-like β-hairpin extension in the NTD clutches RNA molecule by neutralising its phosphate groups, while the base moieties interact with the exposed aromatic residues from the hydrophobic palm.<sup>55</sup> The detailed organisations are by no means resolved.<sup>56</sup>

**The genome – the secret identity**

All CoVs exhibit the same fundamental genomic structure (Figure 11). Therefore, classification is based on their genome sequences. For instance,

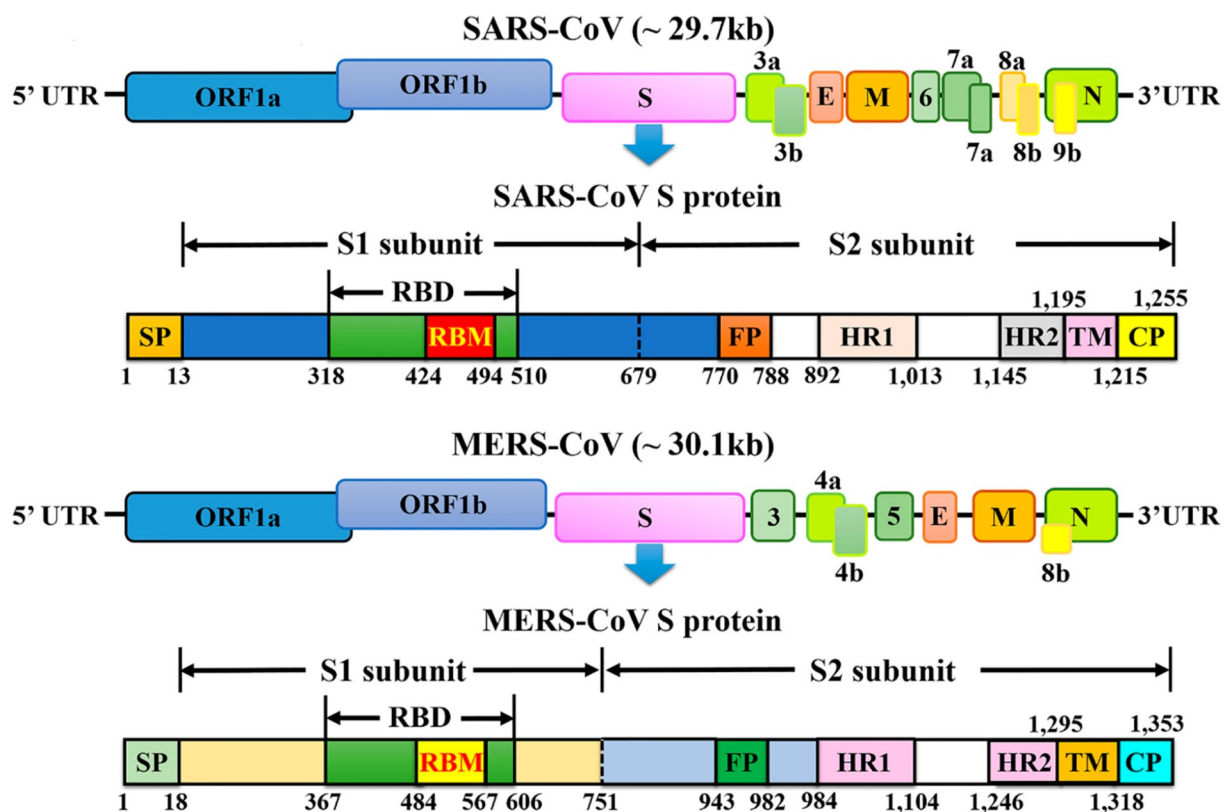


**Figure 10 |** Schematic representation of the genome organization and functional domains of S protein for SARS-CoV and MERS-CoV. (Song *et al. Viruses* 2019, 11(1), 59)

SARS-CoV species are so named not because they cause severe acute respiratory syndrome but that they are genetically related. They may not necessarily cause respiratory illnesses.<sup>57</sup> Specifically, genome analysis based on the rooted phylogeny and calculation of pair-wise evolutionary distances are employed for diagnostic assignments. The key identifiers are conserved domains in replicase polyprotein pp1ab such as ADRP, nsp5 (3CL<sup>pro</sup>), nsp12 (RdRp), nsp13 (Hel), nsp14 (ExoN), nsp15 (NendoU) and nsp16 (O-MT). Ninety percent similarity in the amino acid sequences is considered as the standard species delimitation criterion.<sup>58</sup>

Coronaviruses are positive-sense, single-stranded RNA, or (+)ssRNA, viruses. They are extraordinary among all RNA viruses in that they possess the largest genomes. Their genomes typical range in size from 27,317 nt (HCoV-229E) to 31,357 nt (MHV-A59) in length, in contrast to 10,000 nt in typical RNA viruses. The gammacoronavirus, Beluga whale coronavirus with 31,686 nucleotides in its genome is the largest RNA virus known so far.<sup>59</sup> SAR-CoV-2 has a whole genome of 29,903 nucleotides.<sup>60</sup> The RNA plays a dual role as translation and transcription machineries. Firstly, it acts as a template during translation and directly translates the polyprotein 1a/1ab (pp1a/pp1ab). The protein product encodes 16 nonstructural proteins (nsps) that eventually give rise to the replication-transcription complex (RTC) in a double-membrane vesicles (DMVs).<sup>61</sup> RTC contains several RNA-processing enzymes including the 3'-5' exoribonuclease of nsp14 which appear to perform a proofreading function of the RTC. This 3'-5' exoribonuclease is unique to CoVs compared to other RNA viruses where they are absent. And this enzyme possible contribute to the large size of the genome. RTC transcribes to produce minus-stranded subgenomic RNAs (sgRNAs). The sgRNAs become templates for the synthesis of subgenomic mRNAs. Thus, all the structural and accessory proteins are translated from the sgRNAs.<sup>62</sup>

The CoV RNA contains a 5' cap structure along with a 3' poly (A) tail, which are crucial to function as an mRNA during translation of the replicase polyproteins. The genome is organised in sequence of 5'-leader-UTR-replicase-S (spike)-E (envelope)-M (membrane)-N (nucleocapsid)-3'UTR-poly (A) tail. The leader sequence consists of 67 nucleotides and is followed by an untranslated region (UTR), which is composed of about 200 to 600 nucleotides. There are six open reading frames (ORFs) that are conserved among the CoVs and arranged in a well-defined sequence, viz. ORFs 1a, ORF 1b, S, E, M, and N. The two ORFs collectively comprise the replicase gene. The replicase gene region covers approximately two-thirds of the genome and codes for nonstructural proteins. The nsp 7 to nsp 16 are involved in RNA synthesis and processing.<sup>63</sup> Four ORFs, S, E, M and N constitute about 10 kb and code for the structural proteins such as spike (S),

membrane (M), envelope (E), and nucleocapsid (N) proteins, respectively. Each species has slight variations, for example, MERS-CoV genome contains at least 10 predicted ORFs which included ORF 3, ORF 4a, ORF 4b, and ORF 5 in addition to the conserved ORFs.<sup>64</sup>

The 3' region covers about a third of the total genome. It contains an UTR covering 280 to 500 nucleotides followed by poly(A) sequence. The poly (A) tail is the most variable nucleotide sequence in different CoVs. A common feature in all CoVs is the presence of an octameric sequence, GGAAGAGC beginning at base 73 to 80 upstream from the poly (A) tail.<sup>65</sup> In MERS-CoV, transcription-regulatory sequences (TRSs: 5'-AACGAA-3') are present at the 3' end of the leader sequence and at different positions upstream of genes. It codes for the structural genes along with four accessory genes. The accessory genes are interspersed within the structural genes and their proteins are mainly involved in the pathogenicity of the virus and have little to do with viral replication.<sup>66</sup>

In spite of their miniature sizes and similar organisations, CoVs are extremely highly variables. The genomes of different CoVs shows 54% identity, with 58% identity on the replicase gene and 43% identity on the structural protein-coding region.<sup>62</sup> This indicates that the structural proteins are less conserved and more prone to mutation, which render them more important to adaptation in new hosts.

### Acknowledgement

Journals access was provided by the Wikipedia Library, Wikimedia Foundation, and N-LIST INFLIBNET, Ministry of Human Resource Development, Government of India.

### References

1. Ruska, E. 1987. The development of the electron microscope and of electron microscopy. *Bioscience Reports*, 7(8):607-629.
2. Ruska, E. 1987. The development of the electron microscope and of electron microscopy (Nobel Lecture). *Angewandte Chemie*, 26(7):595-605.
3. Knoll, M., & Ruska, E. 1932. Das elektronenmikroskop. *Zeitschrift für Physik*, 78(5-6):318-339.
4. Ruska, E. 1934. Über Fortschritte im Bau und in der Leistung des magnetischen Elektronenmikroskops. *Zeitschrift für Physik*, 87(9-10): 580-602.
5. Driest, E., & Müller, H. O. 1935. Elektronenmikroskopische Aufnahmen (Elektronenmikrogramme) von Chitinobjekten. *Zeitschrift*

- für wissenschaftliche Mikroskopie*, 52: 53–57.
6. Marton, L. 1935. La microscopie electronique des objets biologiques. *Bulletin de l'Académie Royale des Sciences de Belgique*, 21: 600–617.
  7. Gelderblom, H. R., & Krueger, D. H. 2014. Helmut Ruska (1908–1973): his role in the evolution of electron microscopy in the life sciences, and especially virology. *Advances in Imaging and Electron Physics*, 182: 1–94.
  8. Borries, B. V., & Ruska, E. 1939. Ein Übermikroskop für Forschungsinstitute. *Naturwissenschaften*, 27(34): 577–582.
  9. Ruska, H., Borries, B. V., & Ruska, E. 1939. Die Bedeutung der übermikroskopie für die Virusforschung. *Archiv für die gesamte Virusforschung*, 1(1): 155–169.
  10. Ruska, E. 1934. Über ein magnetisches Objektiv für das Elektronenmikroskop. *Zeitschrift für Physik*, 89 (1–2): 90–128.
  11. Reagan, R.L., Hauser, J.E., Lillie, M.G., Craige Jr., A.H. 1948. Electron micrograph of the virus of infectious bronchitis of chickens. *The Cornell Veterinarian*, 38(2):190–190.
  12. Reagan, R.L., Brueckner, A.L., Delaplane, J.P. 1950. Morphological observations by electron microscopy of the viruses of infectious bronchitis of chickens and the chronic respiratory disease of turkeys. *The Cornell Veterinarian*, 40(4):384–386.
  13. Reagan, R.L., Brueckner, A.L. 1952. Electron microscope studies of four strains of infectious bronchitis virus. *American Journal of Veterinary Research*, 13(48):417–418.
  14. Domermuth, C.H., Edwards, O.F. 1957. An electron microscope study of chorioallantoic membrane infected with the virus of avian infectious bronchitis. *The Journal of Infectious Diseases*, 1:74–81.
  15. Berry, D.M., Cruickshank, J.G., Chu, H.P., Wells, R.J. 1964. The structure of infectious bronchitis virus. *Virology*, 23(3):403–407.
  16. David-Ferreira, J.F., Manaker, R.A. 1965. An electron microscope study of the development of a mouse hepatitis virus in tissue culture cells. *The Journal of Cell Biology*, 24(1):57–78.
  17. Kendall, E.J., Bynoe, M.L., Tyrrell, D.A. 1962. Virus isolations from common colds occurring in a residential school. *The British Medical Journal*, 2 (5297):82–86.
  18. Tyrrell, D.A., Bynoe, M.L. 1961. Some further virus isolations from common colds. *The British Medical Journal*, 1(5223):393–397.
  19. Hamre, D., Procknow, J.J. 1966. A new virus isolated from the human respiratory tract. *Proceedings of the Society for Experimental Biology and Medicine*, 121(1): 190–193.
  20. Hamre, D., Kindig, D.A., Mann, J. 1967. Growth and intracellular development of a new respiratory virus. *Journal of Virology*, 1(4):810–816.
  21. Almeida, J. D., & Howatson, A. F. 1963. A negative staining method for cell-associated virus. *The Journal of Cell Biology*, 16(3): 616–620.
  22. Almeida, J., Cinader, B., & Howatson, A. 1963. The structure of antigen-antibody complexes: A study by electron microscopy. *The Journal of Experimental Medicine*, 118(3): 327–340.
  23. Berry, D. M., & Almeida, J. D. 1968. The morphological and biological effects of various antisera on avian infectious bronchitis virus. *Journal of General Virology*, 3(1): 97–102.
  24. Tyrrell, D.A., Fielder, M. 2002. *Cold Wars: The Fight Against the Common Cold*. Oxford University Press, Oxford, UK, p. 96.
  25. Almeida, J. D., Tyrrell, D. A. 1967. The morphology of three previously uncharacterized human respiratory viruses that grow in organ culture. *Journal of General Virology*, 1(2):175–178.
  26. Becker, W.B., McIntosh, K., Dees, J.H., Chanock, R.M. 1967. Morphogenesis of avian infectious bronchitis virus and a related human virus (strain 229E). *Journal of Virology*, 1(5):1019–1027.
  27. McIntosh, K., Becker, W.B., Chanock, R.M. 1967. Growth in suckling-mouse brain of “IBV-like” viruses from patients with upper respiratory tract disease. *Proceedings of the National Academy of Sciences USA*, 58(6):2268–2273.
  28. Zhu, N., Zhang, D., Wang, W., Li, X., Yang, B., Song, J., Zhao, X., Huang, B., Shi, W., Lu, R., Niu, P. 2020. A novel coronavirus from patients with pneumonia in China, 2019. *The New England Journal of Medicine*, 328(8):727–733.
  29. Neuman, B.W., Kiss, G., Kunding, A.H., Bhella, D., Baksh, M.F., Connelly, S., Droese, B., Klaus, J.P., Makino, S., Sawicki, S.G., Siddell, S.G. 2011. A structural analysis of M protein in coronavirus assembly and morphology. *Journal of Structural Biology*, 174(1):11–22.
  30. Schoeman, D., Fielding, B.C. 2019. Coronavirus envelope protein: current knowledge. *Virology Journal*, 16(1):69.
  31. Liang, J.Q., Fang, S., Yuan, Q., Huang, M., Chen, R.A., Fung, T.S., Liu, D.X. 2019. N-Linked glycosylation of the membrane protein

- ectodomain regulates infectious bronchitis virus-induced ER stress response, apoptosis and pathogenesis. *Virology*, 531:48–56.
32. Bianchi, M., Benvenuto, D., Giovanetti, M., Angeletti, S., Ciccozzi, M., & Pascarella, S. 2020. Sars-CoV-2 envelope and membrane proteins: Structural differences linked to virus characteristics? *BioMed Research International*, 2020:4389089.
  33. Nal, B., Chan, C., Kien, F., Siu, L., Tse, J., Chu, K., Kam, J., Staropoli, I., Crescenzo-Chaigne, B., Escriou, N., van der Werf, S. 2005. Differential maturation and subcellular localization of severe acute respiratory syndrome coronavirus surface proteins S, M and E. *Journal of General Virology*, 86(5):1423–1434.
  34. Surya, W., Li, Y., Verdià-Bàguena, C., Aguilera, V.M., Torres, J. 2015. MERS coronavirus envelope protein has a single transmembrane domain that forms pentameric ion channels. *Virus Research*, 201:61–66.
  35. DeDiego, M.L., Nieto-Torres, J.L., Jimenez-Guardeño, J.M., Regla-Nava, J.A., Castaño-Rodríguez, C., Fernandez-Delgado, R., Usera, F., Enjuanes, L. 2014. Coronavirus virulence genes with main focus on SARS-CoV envelope gene. *Virus Research*, 194:124–37.
  36. Nieto-Torres, J.L., Verdià-Bàguena, C., Jimenez-Guardeño, J.M., Regla-Nava, J.A., Castaño-Rodríguez, C., Fernandez-Delgado, R., Torres, J., Aguilera, V.M., Enjuanes, L. 2015. Severe acute respiratory syndrome coronavirus E protein transports calcium ions and activates the NLRP3 inflammasome. *Virology*, 485:330–339.
  37. Fehr, A.R., Perlman, S. 2015. Coronaviruses: an overview of their replication and pathogenesis. *Methods in Molecular Biology*, 1282:1–23.
  38. Belouzard, S., Millet, J.K., Licitra, B.N., Whittaker, G.R. 2012. Mechanisms of coronavirus cell entry mediated by the viral spike protein. *Viruses*, 4(6):1011–1033.
  39. Li, F. 2016. Structure, function, and evolution of coronavirus spike proteins. *Annual Review of Virology*, 3:237–261.
  40. Naskalska, A., Dabrowska, A., Szczepanski, A., Milewska, A., Jasik, K.P., Pyrc, K. 2019. Membrane protein of human coronavirus NL63 is responsible for interaction with the adhesion receptor. *Journal of Virology*, 93(19):e00355(1–19).
  41. Chan, J.F.W., Kok, K.H., Zhu, Z., Chu, H., To, K.K.W., Yuan, S., Yuen, K.Y. 2020. Genomic characterization of the 2019 novel human-pathogenic coronavirus isolated from a patient with atypical pneumonia after visiting Wuhan. *Emerging Microbes and Infections*, 9(1):221–236.
  42. Alsaadi, J.E.A., Jones, I.M. 2019. Membrane binding proteins of coronaviruses. *Future Virology*, 14(4):275–286.
  43. Peng, G., Xu, L., Lin, Y.L., Chen, L., Pasquarella, J.R., Holmes, K.V., Li, F. 2012. Crystal structure of bovine coronavirus spike protein lectin domain. *Journal of Biological Chemistry*, 287(50):41931–41938.
  44. Wu, K., Li, W., Peng, G., Li, F. 2009. Crystal structure of NL63 respiratory coronavirus receptor-binding domain complexed with its human receptor. *Proceedings of the National Academy of Sciences USA*, 106(47):19970–19974.
  45. Wan, Y., Graham, R., Baric, R.S., Li, F. 2020. Receptor recognition by the novel coronavirus from Wuhan: An analysis based on decade-long structural studies of SARS coronavirus. *Journal of Virology*, 94(7):e00127(1–20).
  46. Andersen, K.G., Rambaut, A., Lipkin, W.I., Holmes, E.C., Garry, R.F. 2020. The proximal origin of SARS-CoV-2. *Nature Medicine*, 26(4):450–452.
  47. Chen, Y., Guo, Y., Pan, Y., Zhao, Z.J. 2020. Structure analysis of the receptor binding of 2019-nCoV. *Biochemical and Biophysical Research Communications*, 525(1):135–140.
  48. Shi, J., Wen, Z., Zhong, G., Yang, H., Wang, C., Huang, B., Liu, R., He, X., Shuai, L., Sun, Z., Zhao, Y. 2020. Susceptibility of ferrets, cats, dogs, and other domesticated animals to SARS-coronavirus 2. *Science*, 368(6494):1016–1020.
  49. Parry, N.M. 2020. COVID-19 and pets: When pandemic meets panic. *Forensic Science International: Reports*, 2:100090.
  50. Zeng, Q., Langereis, M.A., van Vliet, A.L., Huizinga, E.G., de Groot, R.J. 2008. Structure of coronavirus hemagglutinin-esterase offers insight into corona and influenza virus evolution. *Proceedings of the National Academy of Sciences USA*, 105(26):9065–9069.
  51. Tortorici, M.A., Walls, A.C., Lang, Y., Wang, C., Li, Z., Koerhuis, D., Boons, G.J., Bosch, B.J., Rey, F.A., de Groot, R.J., Veerles, D. 2019. Structural basis for human coronavirus attachment to sialic acid receptors. *Nature Structural and Molecular Biology*, 26(6):481–489.
  52. McBride, R., Van Zyl, M., Fielding, B.C. 2014. The coronavirus nucleocapsid is a multifunctional protein. *Viruses*, 6(8):2991–3018.

53. Cong, Y., Kriegenburg, F., de Haan, C.A., Reggiori, F. 2017. Coronavirus nucleocapsid proteins assemble constitutively in high molecular oligomers. *Scientific Reports*, 7(1): 1–10.
54. Lo, C.Y., Tsai, T.L., Lin, C.N., Lin, C.H., Wu, H.Y. 2019. Interaction of coronavirus nucleocapsid protein with the 5'-and 3'-ends of the coronavirus genome is involved in genome circularization and negative-strand RNA synthesis. *The FEBS Journal*, 286(16):3222–3239.
55. Fan, H., Ooi, A., Tan, Y.W., Wang, S., Fang, S., Liu, D.X., Lescar, J. 2005. The nucleocapsid protein of coronavirus infectious bronchitis virus: crystal structure of its N-terminal domain and multimerization properties. *Structure*, 13(12):1859–1868.
56. Masters, P.S. 2019. Coronavirus genomic RNA packaging. *Virology*, 537:198–207.
57. Wu, Y., Ho, W., Huang, Y., Jin, D.Y., Li, S., Liu, S.L., Liu, X., Qiu, J., Sang, Y., Wang, Q., Yuen, K.Y. 2020. SARS-CoV-2 is an appropriate name for the new coronavirus. *The Lancet*, 395(10228):949–950.
58. Gorbalenya, A.E., Baker, S.C., Baric, R.S., de Groot, R.J., Drosten, C., Gulyaeva, A.A., Haagmans, B.L., Lauber, C., Leontovich, A.M., Neuman, B.W., Penzar, D., Perlman, S., Poon, L.L.M., Samborskiy, D.V., Sidorov, I.A., Sola, I., Ziebuhr, J. 2020. The species *Severe acute respiratory syndrome-related coronavirus*: classifying 2019-nCoV and naming it SARS-CoV-2. *Nature Microbiology*, 5:536–544.
59. Mihindukulasuriya, K.A., Wu, G., Leger, J.S., Nordhausen, R.W., Wang, D. 2008. Identification of a novel coronavirus from a beluga whale by using a panviral microarray. *Journal of Virology*, 82(10):5084–5088.
60. Wu, A., Peng, Y., Huang, B., Ding, X., Wang, X., Niu, P., Meng, J., Zhu, Z., Zhang, Z., Wang, J., Sheng, J. 2020. Genome composition and divergence of the novel coronavirus (2019-nCoV) originating in China. *Cell Host and Microbe*, 27(3):325–328.
61. Cui, J., Li, F., Shi, Z.L. 2019. Origin and evolution of pathogenic coronaviruses. *Nature Reviews Microbiology*, 17(3):181–192.
62. Chen, Y., Liu, Q., Guo, D. 2020. Emerging coronaviruses: genome structure, replication, and pathogenesis. *Journal of Medical Virology*, 92(4):418–423.
63. Snijder, E.J., Decroly, E., Ziebuhr, J. 2016. The nonstructural proteins directing coronavirus RNA synthesis and processing. *Advances in Virus Research*, 96(1):59–126.
64. van Boheemen, S., de Graaf, M., Lauber, C., Bestebroer, T.M., Raj, V.S., Zaki, A.M., Osterhaus, A.D., Haagmans, B.L., Gorbalenya, A.E., Snijder, E.J., Fouchier, R.A. 2012. Genomic characterization of a newly discovered coronavirus associated with acute respiratory distress syndrome in humans. *MBio*, 3(6):e00473(1–12).
65. Yang, D., Leibowitz, J.L. 2015. The structure and functions of coronavirus genomic 3' and 5' ends. *Virus Research*, 206:120–133.
66. Abdel-Moneim, A.S. 2014. Middle East respiratory syndrome coronavirus (MERS-CoV): evidence and speculations. *Archives of Virology*, 159(7):1575–1584.